Journal of Materials Chemistry A

# Surface Ligands Influence the Selectivity of Cation Uptake in Polyoxovanadate-alkoxide Clusters

| | |
|---|---|
| Journal: | *Journal of Materials Chemistry A* |
| Manuscript ID | TA-ART-02-2022-001131.R1 |
| Article Type: | Paper |
| Date Submitted by the Author: | 13-Apr-2022 |
| Complete List of Authors: | Garwick, Rachel; University of Rochester, Department of Chemistry<br>Schreiber, Eric; University of Rochester, Department of Chemistry<br>Brennessel, William; University of Rochester, Department of Chemistry<br>McKone, James; University of Pittsburgh, Chemical and Petroleum Engineering<br>Matson, Ellen; University of Rochester, Chemistry |
| | |

ARTICLE

# Surface Ligands Influence the Selectivity of Cation Uptake in Polyoxovanadate-alkoxide Clusters

Rachel E. Garwick,[‡a] Eric Schreiber,[‡a] William W. Brennessel,[a] James R. McKone,*[b] and Ellen M. Matson*[a]

[l]Received 00th January 20xx,
Accepted 00th January 20xx

DOI: 10.1039/x0xx00000x

The selective uptake of lithium ions is of great interest for chemists and engineers because of the numerous uses of this element for energy storage and other applications. However, increasing demand requires improved strategies for the extraction of this element from mixtures containing high concentrations of alkaline impurities. Here, we study solution phase interactions of lithium, sodium, and potassium cations with polyoxovanadate-alkoxide clusters, $[V_6O_7(OR)_{12}]$ (R = $CH_3$, $C_3H_7$, $C_5H_{11}$), using square wave voltammetry and cyclic voltammetry. In all cases, the most reducing event of the cluster shifts in the positive direction as the ionic radius of the cation decreases, indicating increased stability of the reduced cluster and further suggesting that these assemblies might be useful for the selective uptake of $Li^+$. Exploring the consequence of ligand length, we found that the short-chain cluster, $[V_6O_7(OCH_3)_{12}]$, irreversibly binds $Li^+$ in the presence of excess potassium ($K^+$) and exhibits an electrochemical response in titration experiments similar to that observed upon the addition of $Li^+$ to the POV-alkoxide in the presence of non-coordinating tetrabutylammonium ions. However, in the presence of excess sodium ($Na^+$), the cluster showed only a modest preference for lithium, with exchange between sodium and lithium ions governed by equilibrium. Extending these studies to $[V_6O_7(OC_5H_{11})_{12}]$, we found that the presence of the pentyl ligands allows the assembly to irreversibly bind $Li^+$ in the presence of $Na^+$ or $K^+$. The change in mechanism caused by surface functionalization of the clusters increases the differential binding affinity for more compact cations, translating to improved selectivity for $Li^+$ uptake in these molecular assemblies.

## Introduction

Lithium is an important resource, with a broad range of uses in pharmaceuticals[1], greases[2], and battery technologies[3-5]. Our dependence on this metal is anticipated to increase over the next several decades,[6] requiring improved strategies for the extraction of lithium from natural sources. Unfortunately, the majority of the world's lithium supply is contained in continental brine (e.g. seawater, lake water).[7] This fact renders the development of materials that can selectively bind lithium in the presence of high concentrations of contaminants (e.g. other alkali ions, magnesium) critical for the extraction of this metal (Figure 1).[8] Recently, ion-selective electrodes (ISEs), and specifically solid-contact ion-selective electrodes (SCISEs), have become popular in the field of selective ion uptake. SCISEs often make use of conductive polymers like poly(3-octylthiophene),[9] poly(3,4-ethylenedioxythiophene),[10] and polyaniline[11] (Figure 1, left). However, these materials are prone to degradation due to environmental factors like pH changes caused by $CO_2$ levels in the atmosphere, light irradiation, and high temperatures. This fact limits the long-term stability of devices for ion extraction.[12]

To develop durable platforms capable of selective ion uptake,[12] researchers have turned to the investigation of inorganic materials (Figure 1, middle).[13] Reducible metal oxides are of particular interest, as these materials are widely used in well-established lithium-ion battery (LIB) technologies. These bulk materials undergo the reversible lithium (de)insertion processes necessary for the purification of lithium ions, and they have documented stability after thousands of electrochemical (de)insertion cycles.[14-16] Furthermore, the 1-electron: 1-cation stoichiometry exhibited by these materials renders them efficient for electrochemical uptake of alkali ions.

Among metal oxides, well-defined nanocrystalline materials have been shown to outperform bulk materials in $Li^+$ and $Na^+$ insertion. Their high surface-area-to-volume ratios and structural/morphological regularity allow for improved capacity retention in cycling experiments.[17-21] By extension, atomically-precise, molecular metal oxides may further enhance these electrochemical responses, as cation uptake is limited to the surface of the assembly, rendering charge compensation reactions more efficient and tuneable. One such class of these molecules is polyoxometalates (POMs). POMs are discrete molecular compounds comprising multiple $MO_x$ subunits (typically $W^{VI}$, $Mo^{VI}$, or $V^V$) connected through bridging oxide

[a.] *Department of Chemistry, University of Rochester, Rochester NY 14627, USA*
[b.] *Department of Chemical and Petroleum Engineering, University of Pittsburgh, Pittsburgh, Pennsylvania 15260, USA*
‡ Authors contributed equally
Electronic Supplementary Information (ESI) available: Experimental details, $^1$H NMR spectra and CV of compounds reported, CV and SWV of alkali triflate titrations in MeCN and propylene carbonate, and crystallographic parameters. CCDC 2145391 ($[Li(pc)]_2[V_6O_7(OC_3H_7)_{12}]$) and 2145392 ($[^nBu_2N]_2[V_6O_7(OC_3H_7)_{12}]$). See DOI: 10.1039/x0xx00000x

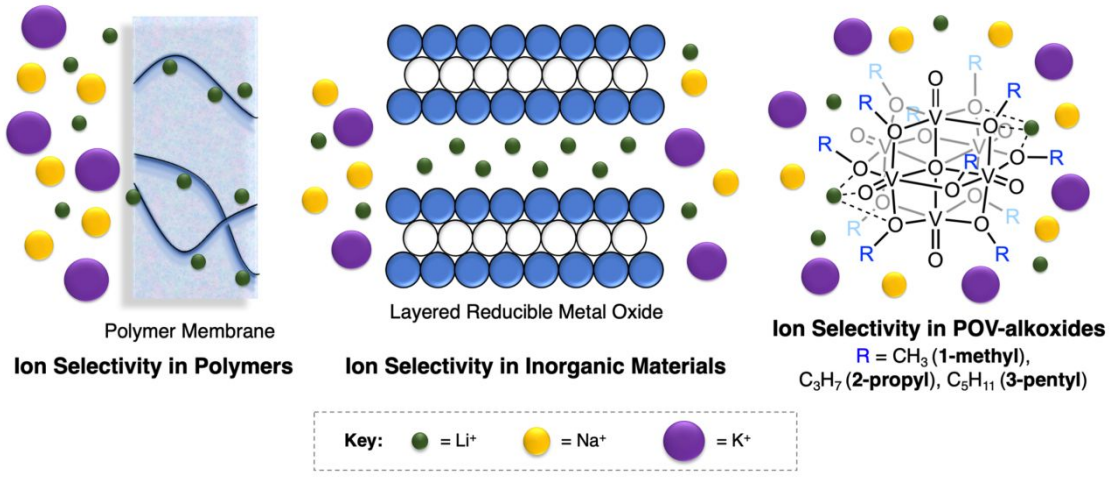


**Figure 1.** Ion selective electrode materials composed of a) polymer electrodes and membranes; b) bulk inorganic materials, and c) atomically precise POV-alkoxides (this work). Purple spheres represent $K^+$ ions, yellow spheres represent $Na^+$ ions, and the green spheres represent $Li^+$ ions.

ligands.[22-25] Indeed, researchers have touted these complexes as molecular models for heterogenous metal oxides due to their structural topology, molecular composition, reducibility, and diffuse electronic structure. With relevance to surface interactions with cations, the reduction of POMs has been shown to be sensitive to the composition of the surrounding electrolyte medium. Protons, alkali, and alkaline earth cations facilitate electron transfer to a given POM at more positive potentials than observed in the presence of outer-sphere charge compensating ions (e.g. tetrabutylammonium, $[^nBu_4N]^+$).[26-30] These studies have led researchers to pose that these clusters could serve as building blocks for atomically precise materials with applications in energy storage.[31, 32] For example, nanostructured POM-hybrid materials have been shown to function as anodes and cathodes in alkali-ion batteries and supercapacitors. Energy losses stemming from internal resistance and structural deformation have been observed, credited to fact that cations need not diffuse through a solid lattice. This allows for $Li^+$ and/or $Na^+$ cycling at high current densities while retaining capacity over prolonged cycling experiments.[33-39]

Recently, our research team reported the effect that alkali ions have on the reduction chemistry of the methoxide bridged POV-alkoxide cluster, $[V_6O_7(OCH_3)_{12}]$, in acetonitrile (MeCN; Figure 1, right).[40] We found that alkali cation-containing electrolytes (MOTf; M= $Li^+$, $Na^+$, $K^+$; OTf = trifluoromethylsulfonate) facilitate the reduction of the cluster at potentials shifted positively in comparison to those observed for the cluster when $[^nBu_4N]$OTf is used as the supporting electrolyte. In particular, the degree of positive shift for the most reducing event ($[V_6O_7(OCH_3)_{12}]^{1-} + e^- \rightarrow [V_6O_7(OCH_3)_{12}]^{2-}$) was found to depend on the size of the cation in the electrolyte. In alkali salt titration experiments, two distinct electrochemical responses were observed: addition of $K^+$ and $Na^+$ resulted in a gradual positive shift of the redox wave; by contrast, addition of $Li^+$ resulted in a distinct electrochemical feature. Characterization of the diltihium salt of the fully reduced POV-alkoxide, $Li_2[V_6O_7(OCH_3)_{12}]$, by single crystal X-ray diffraction, provided additional insight into the nature of the interactions between lithium and the surface of the assembly. $Li^+$ binding was found to be selective for positions on opposing faces of the cluster, whereas larger alkali ions interact with the surface of the cluster at both terminal oxido moieties and at facial sites. Notably, these findings suggest distinct reactivity between $Li^+$ versus other alkali metal cations with the vanadium oxide assembly, thereby motivating further studies on the effect that surface ligands play in directing interactions of metal oxides with alkali ions.

Herein, we expand upon our previous results, and report the investigation of cation interactions of POV-alkoxide clusters functionalized with long-chain surface ligands. The goal of this work is to ascertain how organic functionalization of redox active metal oxides affects cation uptake. The selectivity of cation uptake for the family of complexes is probed through evaluation of the electrochemical response of the clusters in the presence of salt mixtures. It is shown that all clusters evaluated have a thermodynamic preference for $Li^+$ versus $Na^+$ or $K^+$. Comparing electrochemical reduction features reveals that increased ligand bulk about the cluster surface bolsters the differential affinity of the assembly for $Li^+$ ions, resulting in improved selectivity in mixed-salt solutions. These observations suggest that ligand sterics can be used to improve the performance of organofunctionalized POMs in ion-selective, redox active materials and devices.

## Results and Discussion

Previous work describing the effects of alkali ion uptake in $[V_6O_7(OCH_3)_{12}]$ (**1-methyl**) reveals unique regiochemistry and an energetic favourability of $Li^+$ binding to the surface of the cluster upon reduction. This observation led our team to hypothesize that the reduced POV-alkoxide cluster may be capable of selective $Li^+$ uptake in the presence of excess alkali ions as model contaminants. To determine whether the POV-alkoxide

**Scheme 1.** Redox chemistry of $[V_6O_7(OR)_{12}]$.

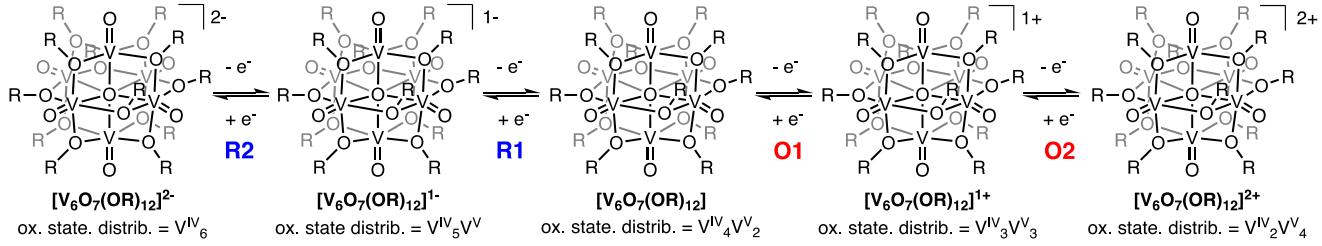


cluster could selectively bind $Li^+$ at low concentrations, we screened the electrochemical behavior of the vanadium oxide assembly in MeCN through a series of titration studies. In these experiments, after recording an initial square-wave voltammogram (SWV) of 1 mM **1-methyl** with 100 mM MOTf (M = $Na^+$, $K^+$) as the supporting electrolyte, a 10 mM solution of LiOTf was titrated into the POV-alkoxide solution (Figure 2; LiOTf added in terms of equivalents per cluster).

In both instances, two electron transfer events were observed; the more positive wave, R1, representing the $[V_6O_7(OCH_3)_{12}] + 1\ e^- \rightleftharpoons [V_6O_7(OCH_3)_{12}]^{1-}$ redox reaction (Scheme 1), was not affected by the addition of LiOTf. In contrast, the more negative process, R2, corresponding to the $[V_6O_7(OCH_3)_{12}]^{1-} + 1\ e \rightleftharpoons [V_6O_7(OCH_3)_{12}]^{2-}$ redox couple (Scheme 1), was sensitive to the addition of $Li^+$ to the salt mixtures.

Upon addition of variable quantities of LiOTf (0.2 to 5 equiv versus 1 mM cluster) in the presence of 100 mM KOTf, the growth of a distinct electrochemical feature at $E_{1/2}$ = -0.471 V (vs $Ag^{+/0}$) is observed (Figure 2c). In previous reporting by our group, this wave was found to correspond with the formation of the reduced, $Li^+$-bound species $Li_2[V_6O_7(OCH_3)_{12}]$ at the electrode surface.[40] The appearance of this event occurs alongside a decrease in the intensity of the original feature corresponding to R2 ($E_{1/2}$ = -0.536 V vs. $Ag^{+/0}$). Following addition of 0.75 equivalents of LiOTf, the $Li^+$-coupled wave completely replaces this original event, indicating that the only species formed upon reduction of the POV-alkoxide to its dianionic state is the $Li^+$ salt. We justify this observation through conditions of the SWV experiments: the dianionic cluster is formed in low concentration only at the electrode surface. As such, the fully reduced cluster is sufficiently selective to scavenge additional $Li^+$ from the electrolyte despite the ready availability of excess $K^+$. As more LiOTf is titrated into solution, R2 continues to shift positively, resulting in an $E_{1/2}$ of -0.409 V (vs $Ag^{+/0}$) at 5 equiv LiOTf. This electrochemical response resembles that noted for the POV-alkoxide upon introduction of $Li^+$ ions with $[^nBu_4N]$OTf as the supporting electrolyte (Figure 2a), and it can be credited to the irreversible uptake of $Li^+$ at the surface of the cluster. Note, however, that the separation between the two $E_{1/2}$ values, $E_{1/2}$ R2(LiOTf) and $E_{1/2}$ R2(KOTf), is less than that observed in the $[^nBu_4N]$OTf/LiOTf mixture, leading to overlap of the $K^+$- and $Li^+$-coupled electrochemical features.

In contrast, addition of LiOTf to **1-methyl** in the presence of 100 mM of NaOTf reveals a more gradual positive shift of R2 (Figure 2b). The initial SWV of $[V_6O_7(OCH_3)_{12}]$ showed R2 with an $E_{1/2}$ at -0.451 V (vs $Ag^{+/0}$). As a 10 mM solution of LiOTf was titrated (0.2 to 5.0 equiv compared to moles of cluster), R2 shifts to $E_{1/2}$ value of -0.400 V (vs $Ag^{+/0}$).

Both experiments indicate that the fully reduced form of the POV-alkoxide is preferentially stabilized by $Li^+$. However, the extent of this stabilization gives rise to characteristic differences observed in the titration experiments. Specifically, the $E_{1/2}$ value of R2 shifted by $\Delta E_{K\rightarrow Li} = 232$ mV when $K^+$ was replaced by $Li^+$ as the predominant charge-compensating cation (Table 1). This shift was sufficient to result in rapid, chemically irreversible binding of $Li^+$ upon reduction, as evidenced by the emergence of a completely new voltametric feature even in the presence of substoichiometric $Li^+$. By contrast, the shift $\Delta E_{Na\rightarrow Li}$ was only

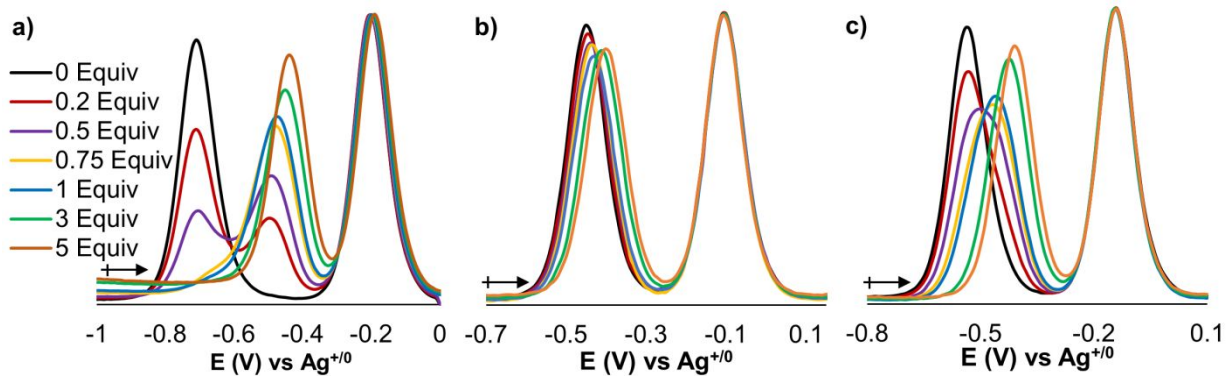


**Figure 2.** SWVs of LiOTf titration experiments to 1 mM solutions of **1-methyl** in MeCN with 100 mM of a) $[^nBu_4N]$OTf , b) NaOTf, or c) KOTf as the supporting electrolyte. Equivalents of LiOTf are relative to the concentration of **1-methyl**.

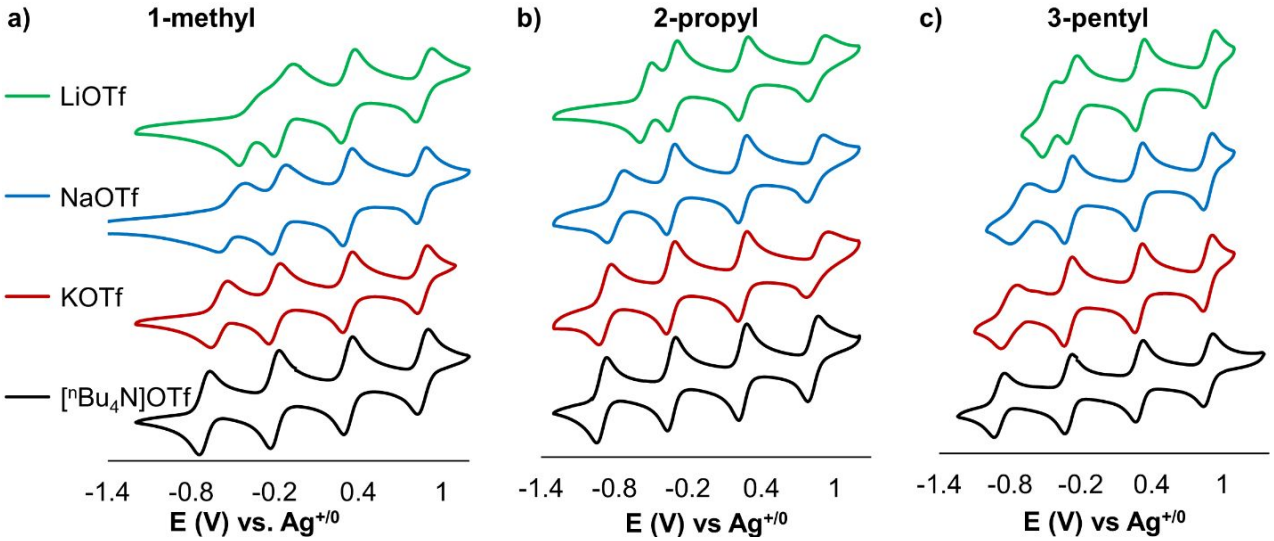


**Figure 3.** CVs of 1 mM solutions of complexes a) $[V_6O_7(OCH_3)_{12}]$ (**1-methyl**), b) $[V_6O_7(OC_3H_7)_{12}]$ (**2-propyl**), and c) $[V_6O_7(OC_5H_{11})_{12}]$ (**3-pentyl**) collected in MeCN with 100 mM supporting electrolyte (Blue = $[^nBu_4N]OTf$, Red = LiOTf, Purple = NaOTf, Green = KOTf) at a scan rate of 100 $mVs^{-1}$.

**Table 1.** Electrochemical parameters of complexes $[V_6O_7(OCH_3)_{12}]$ (**1-methyl**), $[V_6O_7(OC_3H_7)_{12}]$ (**2-propyl**), and $[V_6O_7(OC_5H_{11})_{12}]$ (**3-pentyl**) in MeCN with various supporting electrolytes (MOTf; M = $[^nBu_4N]^+$, $Li^+$, $Na^+$, $K^+$)

| Compound | Redox Event | [nBu4N][OTf][a] | | LiOTf[a] | | | NaOTf[a] | | KOTf[a] | |
|---|---|---|---|---|---|---|---|---|---|---|
| | | $E_{1/2}$ | $\Delta E_p$ | $E_{1/2}$ | $\Delta E_p$ | $\Delta E_{1/2}$[b] | $E_{1/2}$ | $\Delta E_p$ | $E_{1/2}$ | $\Delta E_p$ |
| **1-methyl** | R1 | -0.198 V | 60 mV | -0.130 V | 142 mV | -- | -0.169 V | 105 mV | -0.202 V | 82mv |
| | R2 | -0.703 V | 68 mV | -0.3615 V[c] | 198 mV[c] | 0.341 V[c] | -0.507 V | 189 mV | -0.594 V | 119 mv |
| **2-propyl** | R1 | -0.330 V | 67 mV | -0.320 V | 74 mV | -- | -0.330 V | 68 mV | -0.330 V | 70 mV |
| | R2 | -0.902 V | 81 mV | -0.544 V | 96 mV | 0.358 V | -0.760 V | 138 mV | -0.859 V | 103 mV |
| **3-pentyl** | R1 | -0.304 V | 64 mV | -0.289 V | 87 mV | 0.015 V | -0.303 V | 71 mV | -0.307 V | 71 mV |
| | R2 | -0.890 V | 80 mV | -0.470 V | 112 mV | 0.420 V | -0.710 V | 118 mV | -0.811 V | 120 mV |

[a]All redox couples are reported vs. $Ag^{+/0}$. [b] Difference in $E_{1/2}$ between R2 of cluster with $[^nBu_4N]OTf$ and LiOTf as the support electrolyte. [c] The anodic sweep of R2 overlaps with that of R1 when LiOTf is used as a supporting electrolyte in the case of **1-methyl**; $E_{1/2}$ and $\Delta E_p$ are reported as best approximations.

145 mV when $Na^+$ was replaced by $Li^+$, and the peak shifts gradually with further additions of $Li^+$, implying chemically reversible coordination of alkali ions to the cluster surface (i.e. an equilibrium between $Li_2[V_6O_7(OCH_3)_{12}]$ and $Na_2[V_6O_7(OCH_3)_{12}]$; Table 1). These results indicate that the selectivity of the complex toward $Li^+$ uptake will also be considerably diminished in the presence of $Na^+$ containing electrolytes compared to those containing $K^+$.

Interested in further modifying the selectivity of cation uptake in POV-alkoxide clusters, we turned our attention to chemical modification of the surface of the assembly. We hypothesized that by altering the ligands on the POV-alkoxide, interactions of alkali ions with the surface of the cluster would be affected, thus influencing the overall selectivity of the assembly for $Li^+$. We reasoned that increased steric incumbrance imparted by longer alkyl groups on the cluster surface should weaken outer-sphere charge compensating interactions, such as those observed in the case of the POV-alkoxide cluster with $Na^+$ and $K^+$; whereas coordination of the strongest-binding alkali ion, $Li^+$, would be independent of ligand length as a result of its tight and specific binding motif.

To test our hypothesis, electrochemical analyses of a series of complexes with the general formula $[V_6O_7(OR)_{12}]^n$, herein named **1-methyl** (R = $CH_3$), **2-propyl** (R = $C_3H_7$), and **3-pentyl** (R = $C_5H_{11}$), were performed. The selected assemblies possess bridging alkoxide ligands of varying lengths. Notably, these modifications do not significantly impact the electronics of the cluster core.[41-43] CV experiments were conducted with each cluster dissolved in MeCN in the presence of 100 mM MOTf (M = $[^nBu_4N]^+$, $K^+$, $Na^+$, $Li^+$) as the supporting electrolyte (Figure 3, Table 1). As observed in previous reporting from our group, only the $E_{1/2}$ of the most reducing wave (R2; Scheme 1) for all three complexes was found to be sensitive to the identity of the electrolyte cation, with the electrochemical event shifting positively in the order $K^+ < Na^+ < Li^+$ as compared to $[^nBu_4N]^+$.

Further analysis of the CVs reveals that surface ligands have little impact on the positive shift and reversibility of the most reducing wave for the cluster series in the presence of both $Na^+$ and $K^+$ ions (Table 1). This observation is further evidence for non-specific binding of these ions at the cluster surface upon reduction, with charge compensation ultimately governed by outer-sphere interactions. The increased alkyl-chain length decreases the influence of the alkali ion on the electrochemistry

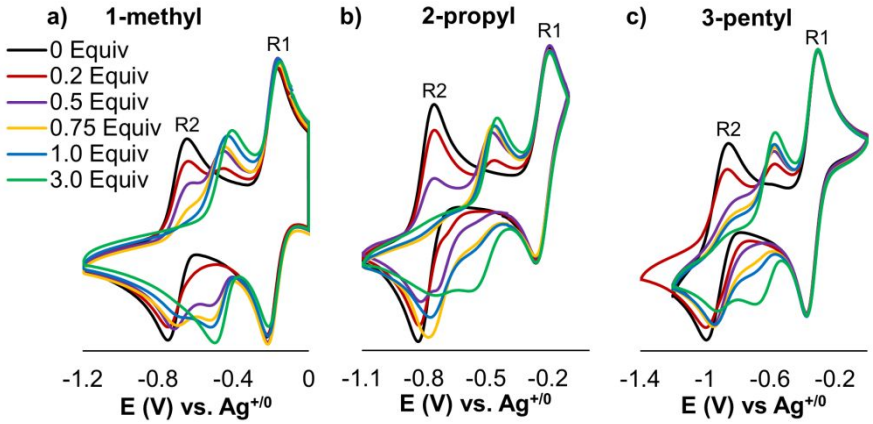


**Figure 4.** CV data from titration of LiOTf into 1 mM solutions of a) **1-methyl**, b) **2-propyl**, and c) **3-pentyl** in MeCN with 100 mM [$^n$Bu$_4$N]OTf supporting electrolyte, collected at 100 mVs$^{-1}$. Equivalents listed are with respect to cluster concentration.

of the vanadium oxide core. MOTf (M = Na$^+$ and K$^+$) titration experiments also supported this nonspecific binding mode; in analogy to results reported for similar experiments with **1-methyl**, gradual positive shifts in R2 were observed for both **2-propyl** and **3-pentyl** with respect to MOTf concentration (Figure S7-S8).

On the other hand, the redox properties of the series of clusters with LiOTf as the supporting electrolyte reveal several intriguing trends. First, the positive shift in reduction potential, $\Delta E_{nBu\rightarrow Li}$, for R2 between [$^n$Bu$_4$N]OTf and LiOTf for the cluster series was observed to be influenced by alkoxide chain length. Increased ligand chain length produced a larger positive shift in R2, such that $\Delta E_{nBu\rightarrow Li}$ of **1-methyl** (0.341 V) < **2-propyl** (0.358 V) < **3-pentyl** (0.420 V), suggesting a thermodynamic preference for Li$^+$ binding over clusters with shorter surface ligands. In addition, the apparent reversibility, represented by the difference in voltage of the cathodic and anodic half-wave potentials, $\Delta E_p$, of this redox process, in the presence of LiOTf was found to be improved for the long-chain clusters (Table 1).

To probe the interactions of the reduced clusters in the presence of substoichiometric amounts of LiOTf, titration of this salt into an electrochemical cell containing 1 mM of cluster and 100 mM [$^n$Bu$_4$N]OTf in MeCN was performed. For all three complexes, substoichiometric addition of LiOTf resulted in the growth of a new electrochemical event at a more positive potential with respect to R2 in the presence of the tetrabutylammonium electrolyte (Figure 4). As Li$^+$ equivalents are added, the new wave replaces the initial reduction feature. Previously, we attributed this response to the specific binding of Li$^+$ ions to the surface of **1-methyl** upon reduction, whereby the bound cations are located at opposing faces of the POV-alkoxide. These titration results suggest that the Li$^+$ binding mode is conserved across all three complexes.

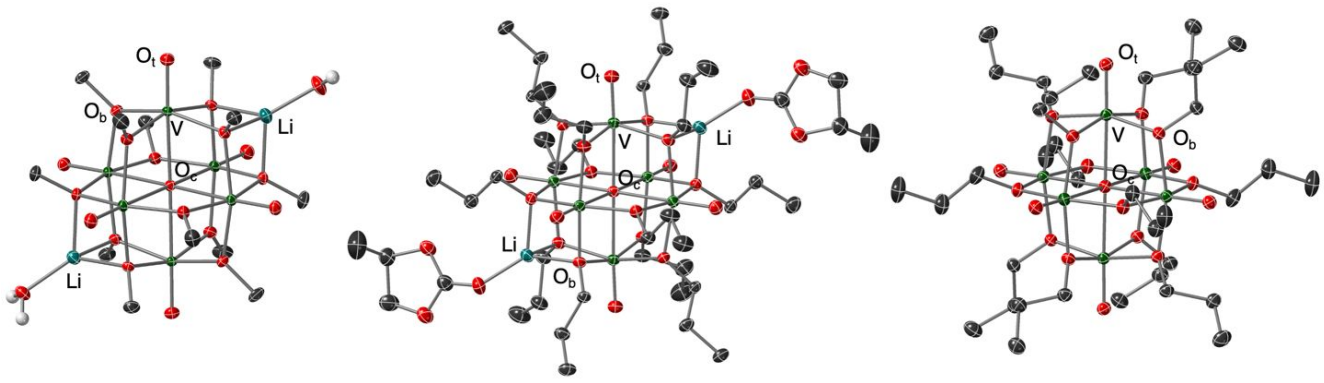


**Figure 5.** Molecular structures of $[Li(OH_2)]_2[V_6O_7(OCH_3)_{12}]$ ([Li(OH$_2$)]$_2$[**1-methyl**]), $[Li(pc)]_2[V_6O_7(OC_3H_7)_{12}]$ ([Li(pc)]$_2$[**2-propyl**]), and $[^nBu_4N]_2[V_6O_7(OC_3H_7)_{12}]$ ([$^n$Bu$_4$N]$_2$[**2-propyl**]) shown with 30% probability ellipsoids. Hydrogen atoms, solvent molecules, and tetrabutylammonium ions have been removed for clarity.

**Table 2.** Structural parameters of $[Li(OH_2)]_2[V_6O_7(OCH_3)_{12}]$[40] ([Li(OH$_2$)]$_2$[**1-methyl**]), $[^nBu_4N]_2[V_6O_7(OCH_3)_{12}]$[40] ([$^n$Bu$_4$N]$_2$[**1-methyl**]), $[Li(pc)]_2[V_6O_7(OC_3H_7)_{12}]$ (Li$_2$[**2-propyl**]), and $[^nBu_4N]_2[V_6O_7(OC_3H_7)_{12}]$ ([$^n$Bu$_4$N]$_2$[**2-propyl**]).

| Bond | [Li(OH$_2$)]$_2$[1-methyl] | [$^n$Bu$_4$N]$_2$[1-methyl] | [Li(pc)]$_2$[2-propyl] | [$^n$Bu$_4$N]$_2$[2-propyl] |
|---|---|---|---|---|
| Li-O$_b$[b] (avg) | 1.9653 Å | -- | 1.964 Å | -- |
| V=O$_t$[d] (avg) | 1.6054 Å | 1.606 Å | 1.6035 Å | 1.6123 Å |
| V-O$_c$[e] | 2.3191 Å | 2.311 Å | 2.3198 Å | 2.3167 Å |
| V-O$_b$[b] (avg; no M$^+$) | 1.9889 Å | 1.999 Å | 1.9914 Å | 2.0127 Å |
| V-O$_b$[b] (avg; M$^+$-bound) | 2.0360 Å | -- | 2.0580 Å | -- |

As previously described by our research group, exposure of the fully reduced complex $[^nBu_4N]_2$[**1-methyl**] to LiOTf in MeCN generates the $Li^+$ salt as an insoluble powder.[40] Similar experiments with dianionic **2-propyl** and **3-pentyl** were performed; however, these clusters remained soluble in MeCN in the presence of LiOTf. An alternative method was developed to isolate the reduced, lithiated salt of **2-propyl**, wherein the independently synthesized, reduced species $[^nBu_4N]_2$[**2-propyl**] was dissolved in propylene carbonate and combined with a solution of lithium bis(trifluoromethylsulfonyl)imide in diethyl ether. Note that analogous titration experiments in propylene carbonate reveal similar electrochemical response to those in MeCN, which is expected given the similar donor numbers of both solvents (Figure S9).[44] Once combined, toluene and pentane were added, from which teal crystals suitable for analysis by single crystal X-ray diffraction can be isolated.

Refinement of crystallographic data reveals the product as the $Li^+$ salt of the reduced, propoxide-bridged complex (Figure 5, Table 2). Like its methoxide-substituted congener, two $Li^+$ ions occupy binding sites on opposite faces of the assembly. To draw comparisons between the lithium adduct of the propoxide-bridged POV-alkoxide cluster and the tetrabutylammonium salt of the dianionic assembly, crystals were also obtained of $[^nBu_4N]_2$[**2-propyl**] (Figure 5, Table 2). Despite the overall retention of the Lindqvist core structure, the installation of $Li^+$ on the face of the assembly results elongations of the associated V-$O_b$ bonds in $[Li(pc)]_2$[**2-propyl**] with respect to the parent dianion (2.0580 vs 2.0127 Å; $O_b$ = O atom of the bridging alkoxide ligand). Truncation of V-$O_b$ bonds that do not feature a bound $Li^+$ ion was also observed (1.9914 Å); this is a consequence of the *trans* effect across the individual vanadium ions of the $VO_6$ pseudo-octahedra. These bond perturbations are concomitant with a rearrangement of the organic moieties on the cluster surface, which are all angled outward from the $Li^+$ ion on the bridging oxide face. In the case of the $[^nBu_4N]^+$ salt, the propyl chains are not constrained to a single orientation about the vanadium oxide core. Similar structural observations have been noted for the analogous dianions of **1-methyl**. We expect that a similar structure is formed upon reduction of **3-pentyl** in the presence of $Li^+$-containing electrolyte.

These structural details, along with voltammetry data, show that the binding mode of alkali cations is conserved across the POV-alkoxide series. Hence, changes in binding mode do not play an additional role in increasing the selectivity of the longer-chain POV-alkoxides. However, the observed thermodynamic advantage of $Li^+$ binding to sterically encumbered clusters suggests that decoration of the POV-alkoxide surface with long-chain alkyl substituents affects the relative energetics and intermolecular interactions for ion pair formation. This point may serve to further enhance the selectivity of POV-alkoxide assemblies for $Li^+$ ion uptake. Despite an apparent kinetic barrier to $Li^+$ coordination in the presence of $[^nBu_4N]$OTf, the increased ligand sphere of **3-pentyl** results in a greater thermodynamic driving force for the formation of $Li_2$[**3-pentyl**] at the electrode surface over analogous ion pairs with **1-methyl** and **2-propyl**. The bulky surface groups shield the bound cation, forcing it to more closely associate with the negatively charged cluster core, thereby supporting its formation at a more anodic potential. In addition, the non-specific binding of $K^+$ and $Na^+$ is further disfavoured by the incorporation of nonpolar groups on the cluster surface that forces these solvated ions further from the cluster core. This yields a strained ion pairing motif which requires more cathodic potentials to be formed.

To assess how this information informs the selectivity of $Li^+$ ion uptake on long-chain POV-alkoxide clusters, we next performed electrochemical measurements in salt mixtures with **3-pentyl** (Figure 6). Titration of LiOTf into a solution of **3-pentyl** in MeCN with KOTf as the supporting electrolyte yields a similar response to that observed for **1-methyl** (Figure 6c): the addition of substoichiometric amounts of LiOTf (0.2 equiv) results in a decrease in R2 ($E_{1/2}$ = -0.841 V vs $Ag^{+/0}$) concomitant with the appearance of a new event ($E_{1/2}$ =-0.603 V vs $Ag^{+/0}$). By the addition of 0.5 equiv of LiOTf, R2 was completely replaced by the $Li^+$-coupled redox event. Subsequent addition of LiOTf (up to 5 equiv) results in an additional positive shift of this new redox event to an $E_{1/2}$ of -0.590 V (vs $Ag^{+/0}$). Despite the analogous electrochemical response between **1-methyl** and **3-pentyl** in the presence of $Li^+/K^+$ salt mixtures, these results are differentiated by the magnitude of the positive shift in reduction potential at the beginning and end of the titration experiment. This change in potential upon addition of 5 equiv

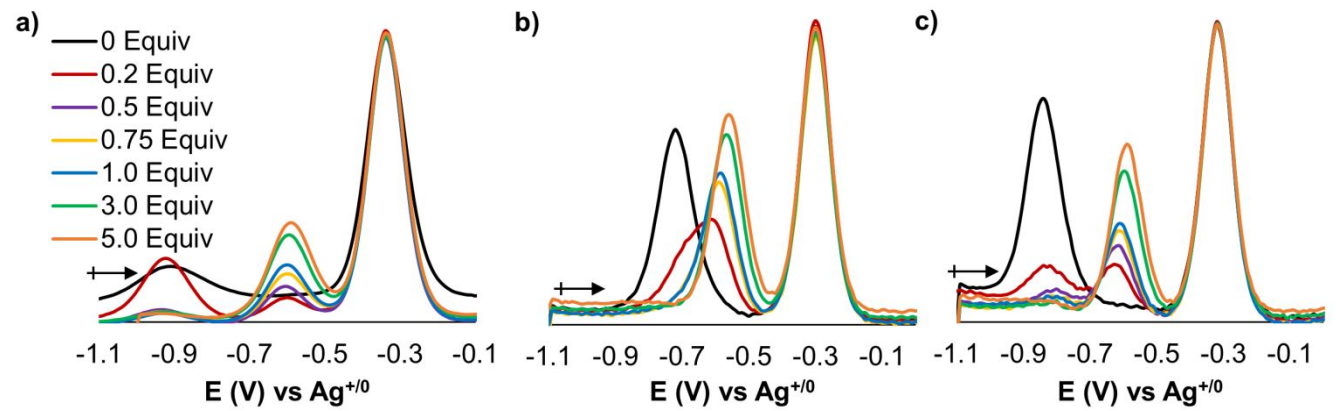


**Figure 6.** SWV of $Li^+$ selectivity experiments with 1 mM **3-pentyl** with 100 mM of a) $[^nBu_4N]$OTf , b) NaOTf, or c) KOTf as the supporting electrolyte. Equivalents of LiOTf are relative to the concentration of **3-pentyl**.

of LiOTf was 162 mV for **1-methyl** and 251 mV for **3-pentyl**. This discrepancy suggests a significant energetic advantage to $Li^+$ salt formation upon reduction of **3-pentyl** over **1-methyl**, even in a 20-fold excess of $K^+$ ions.

Further demonstration of the improved ion selectivity of the pentoxide-bridged assembly was obtained through titration experiments involving the addition of LiOTf into a solution of **3-pentyl** in NaOTf electrolyte (Figure 6b). Upon addition of 0.2 equiv of LiOTf, the initial R2 wave at $E_{1/2}$ = -0.722 V (vs $Ag^{+/0}$), shifted to approximately -0.700 V (vs $Ag^{+/0}$) and also developed an asymmetric shape, suggesting the formation of a new electrochemical process centred at -0.612 V (vs $Ag^{+/0}$). The growth of this wave suggests that the formation of the $Li^+$ salt is competitive with the generation of an equilibrium of alkali salts at low LiOTf concentration. To confirm the hypothesized mixture of redox waves between -0.700 and -0.600 V (vs $Ag^{+/0}$), titrations were performed with still smaller amounts of LiOTf, wherein it was observed that upon addition of as little as 0.05 equiv LiOTf, R2 was broadened with the growth of this $Li^+$ coordination event (Figure 7). Upon the addition of 0.2 equiv LiOTf, the $Li^+$-coupled wave predominated in this voltage range. Further addition of the alkali titrant led to the complete consumption of the initial reduction wave in favour of selective $Li^+$ binding by only 1 equiv of LiOTf. This response contrasts with the equilibrium observed in analogous experimentation with **1-methyl**. These experiments confirm that, even in a 100-fold excess of $[^nBu_4N]^+$, $K^+$, or $Na^+$ over $Li^+$ ions, **3-pentyl** is fully selective for $Li^+$ ion uptake upon complete reduction.

We propose that the difference in cation selectivity between **1-methyl** and **3-pentyl** results from the relative thermodynamics of charge compensation and rapid reaction rate relative to the electrochemical time scales accessed herein (*vide supra*). Titration of LiOTf into a solution of **1-methyl** using NaOTf as the supporting electrolyte results in a gradual shift in the potential of R2 to more positive potentials, indicating an equilibrium in solution containing alkali-bound complexes of the form $M_2$[**1-methyl**], where M = $Li^+$ and $Na^+$. However, addition of LiOTf into a solution of **1-methyl** in KOTf electrolyte resulted in the replacement of R2 with a new event entirely, indicating that the reformation of $K_2$[**1-methyl**] does not proceed at appreciable rates even in the presence of superstochiometric amounts of $K^+$ ions. These disparate responses are due to the magnitude of difference between R2 of **1-methyl** in KOTf or NaOTf versus LiOTf ($\Delta E_{M\rightarrow Li}$ = 0.232 V and 0.146 V when M = $K^+$ and $Na^+$, respectively; Table 1). These voltage differences can be interpreted as the driving force for $Na^+$ or $K^+$ substitution by $Li^+$. Because this difference is smaller for NaOTf, the energetic advantage for the formation of the $Li^+$ salt of the short-chained cluster is insufficient to facilitate irreversible binding, resulting in an equilibrium mixture. On the other hand, the larger $\Delta E_{1/2}$ with KOTf versus LiOTf suggests a threshold magnitude in $\Delta E_{M\rightarrow Li}$ for R2 exists for accessing the irreversible binding of $Li^+$, located somewhere between 0.15 and 0.23 V.

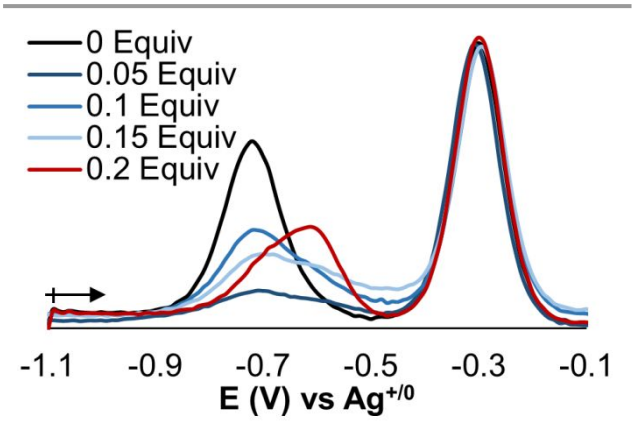


**Figure 7.** SWV of titration experiments: substoichiometric amounts of LiOTf added to a solution of 1 mM **3-pentyl** with 100 mM NaOTf as the supporting electrolyte. Equivalents of LiOTf added are with respect to cluster.

On the other hand, LiOTf titrations into both NaOTf and KOTf electrolyte solutions of **3-pentyl** result in irreversible $Li^+$ binding. This is consistent with the observed magnitude of $\Delta E_{Li\rightarrow M}$ for both these electrolytes with respect to LiOTf (0.240 V and 0.341 V for M = Na and K, respectively). Both of these values are greater than the maximum 0.230 V observed for **1-methyl**, indicating that the energetic advantage for the formation of the lithium adduct of the long-chained cluster is sufficient to support rapid, quantitative uptake of $Li^+$, even at low relative $Li^+$ concentrations. This was demonstrated most strikingly in the titration of LiOTf into a solution of **3-pentyl** with NaOTf as the supporting electrolyte; complete $Li^+$ ion selectivity was achieved in a 100:1 $Na^+$:$Li^+$ salt mixture (Figure 7).

## Conclusions

This work demonstrates that straightforward molecular modifications can be used to improve the selectivity of alkali ion uptake upon the electrochemical reduction of metal oxide assemblies. Initial results showed that the methoxide-bridged POV-alkoxide **1-methyl** is selective for $Li^+$ over $[^nBu_4N]^+$ and $K^+$ ions, but $Na^+$ binding is competitive with $Li^+$. Increasing the steric bulk by using primary alkoxides with longer aliphatic chains further destabilizes the binding of $Na^+$ and $K^+$ relative to $Li^+$, due in large part to the different binding mode of alkali ions. This is due to the observation that $Na^+$ and $K^+$ ions coordinate non-specifically to the reduced Lindqvist core, whereas $Li^+$ binds regioselectively, with two cations coordinated on opposing faces of the cluster. These ion pairing interactions are conserved across the series of alkoxide-bridged clusters, meaning that the change in cation selectivity depends not on fundamental changes cation binding mode, but instead on surface ligand chain length. The thermodynamic preference for $Li^+$ uptake in the case of the pentanol-derived cluster, **3-pentyl**, over $Na^+$ and $K^+$ translates into significant improvements in $Li^+$ ion selectivity at low $Li^+/K^+$ and $Li^+/Na^+$ ratios.

These results indicate that modulation of ligand sterics can be used as a general strategy to manipulate the selectivity of cation uptake on molecular metal oxide clusters, providing a possible avenue for application of these complexes in electrochemical devices for $Li^+$ separation from salt mixtures. In this context, a key challenge in the extraction of $Li^+$ from terrestrial brines its selective uptake over $Mg^{2+}$ ions in aqueous

solution.[45-48] This motivates additional work to understand how ligand design impacts selectivity for mono versus divalent cations, and to learn how to make these types of complexes compatible with aqueous environments.

## Author Contributions

R.E.G. and E.S. conducted all synthetic and electrochemical experiments and interpreted results. W.W.B. collected single crystal X-ray diffraction data and refined both crystal structures. E.M.M. directed the project in consultation with J.R.M. The manuscript was written through contributions of all authors. All authors have given approval for the final version of the manuscript.

## Conflicts of interest

The authors declare no competing financial interest.

## Acknowledgements

The authors acknowledge Prof. Timothy R. Cook for helpful discussions. This research was funded by the National Science Foundation, Division of Chemical, Bioengineering, Environmental, and Transport Systems Program (Award 2015749). R.E.G., E.S., and E.M.M. were also supported by program manager Dr. Imre Gyuk through the U.S. Department of Energy, Office of Electricity Delivery and Energy Reliability. R.E.G. is a recipient of a Graduate Research Fellowship from the National Science Foundation.

## Notes and references

1. T. Sakata, M. Hagio, A. Saito, Y. Mori, M. Nakao and K. Nishi, *Sci Technol Adv Mater*, 2020, **21**, 379-387.
2. L. T. Peiro, G. V. Mendez and R. U. Ayres, *Jom-Us*, 2013, **65**, 986-996.
3. B. Dunn, H. Kamath and J. M. Tarascon, *Science*, 2011, **334**, 928-935.
4. P. Cui, Q. Zhang, C. Sun, J. Gu, M. X. Shu, C. Q. Gao, Q. Zhang and W. Wei, *Rsc Adv*, 2022, **12**, 3828-3837.
5. Y. H. Zhu, Y. Han, Q. P. Guo, H. Wang, H. Z. Jiang, H. L. Jiang, W. W. Sun, C. M. Zheng and K. Xie, *Electrochim Acta*, 2021, **394**.
6. G. Berckmans, M. Messagie, J. Smekens, N. Omar, L. Vanhaverbeke and J. Van Mierlo, *Energies*, 2017, **10**.
7. X. H. Li, Y. H. Mo, W. H. Qing, S. L. Shao, C. Y. Y. Tang and J. X. Li, *J Membrane Sci*, 2019, **591**.
8. L. C. Zhang, L. J. Li, D. Shi, J. F. Li, X. W. Peng and F. Nie, *Sep Purif Technol*, 2017, **188**, 167-173.
9. N. Rubinova, K. Chumbimuni-Torres and E. Bakker, *Sensor Actuat B-Chem*, 2007, **121**, 135-141.
10. M. Vazquez, J. Bobacka, A. Ivaska and A. Lewenstam, *Sensor Actuat B-Chem*, 2002, **82**, 7-13.
11. T. Lindfors and A. Ivaska, *Anal Chem*, 2004, **76**, 4387-4394.
12. T. Lindfors, *J Solid State Electr*, 2009, **13**, 77-89.
13. S. Komaba, T. Akatsuka, K. Ohura, C. Suzuki, N. Yabuuchi, S. Kanazawa, K. Tsuchiya and T. Hasegawa, *Analyst*, 2017, **142**, 3857-3866.
14. S. Fang, D. Bresser and S. Passerini, *Advanced Energy Materials*, 2020, **10**, 1902485.
15. J. Jiang, Y. Li, J. Liu, X. Huang, C. Yuan and X. W. D. Lou, *Advanced Materials*, 2012, **24**, 5166-5180.
16. Z. S. Wu, G. M. Zhou, L. C. Yin, W. Ren, F. Li and H. M. Cheng, *Nano Energy*, 2012, **1**, 107-131.
17. Y. N. Xu, Q. L. Wei, C. Xu, Q. D. Li, Q. Y. An, P. F. Zhang, J. Z. Sheng, L. Zhou and L. Q. Mai, *Advanced Energy Materials*, 2016, **6**.
18. A. Q. Pan, J. G. Zhang, Z. M. Nie, G. Z. Cao, B. W. Arey, G. S. Li, S. Q. Liang and J. Liu, *J Mater Chem*, 2010, **20**, 9193-9199.
19. G. Armstrong, J. Canales, A. R. Armstrong and P. G. Bruce, *J Power Sources*, 2008, **178**, 723-728.
20. M. F. Oszajca, M. I. Bodnarchuk and M. V. Kovalenko, *Chem Mater*, 2014, **26**, 5422-5432.
21. Y. Y. Yang, Y. Q. Zhao, L. F. Xiao and L. Z. Zhang, *Electrochem Commun*, 2008, **10**, 1117-1120.
22. L. Cronin and A. Muller, *Chem Soc Rev*, 2012, **41**, 7333-7334.
23. D. L. Long, E. Burkholder and L. Cronin, *Chem Soc Rev*, 2007, **36**, 105-121.
24. M. T. Pope, *Heteropoly and isopoly oxometalates*, Springer-Verlag, Berlin ; New York, 1983.
25. M. T. M. Pope, A., *Polyoxometalate Chemistry From Topology via Self-Assembly to Applications*, 2001.
26. J. M. Gomez-Gil, E. Laborda, J. Gonzalez, A. Molina and R. G. Compton, *J Phys Chem C*, 2017, **121**, 26751-26763.
27. S. Himeno, M. Takamoto and T. Ueda, *J Electroanal Chem*, 2000, **485**, 49-54.
28. M. Takamoto, T. Ueda and S. Himeno, *J Electroanal Chem*, 2002, **521**, 132-136.
29. T. Konishi, K. Kodani, T. Hasegawa, S. Ogo, S. X. Guo, J. F. Boas, J. Zhang, A. M. Bond and T. Ueda, *Inorg Chem*, 2020, **59**, 10522-10531.
30. T. Ueda, K. Kodani, H. Ota, M. Shiro, S. X. Guo, J. F. Boas and A. M. Bond, *Inorg Chem*, 2017, **56**, 3990-4001.
31. S. Uchida, *Chem Sci*, 2019, **10**, 7670-7679.
32. T. Ueda, *Chemelectrochem*, 2020, **7**, 2888-2888.
33. J. J. Chen, M. D. Symes, S. C. Fan, M. S. Zheng, H. N. Miras, Q. F. Dong and L. Cronin, *Advanced Materials*, 2015, **27**, 4649-4654.
34. J. J. Chen, J. C. Ye, X. G. Zhang, M. D. Symes, S. C. Fan, D. L. Long, M. S. Zheng, D. Y. Wu, L. Cronin and Q. F. Dong, *Advanced Energy Materials*, 2018, **8**.
35. B. Iqbal, X. Y. Jia, H. B. Hu, L. He, W. Chen and Y. F. Song, *Inorg Chem Front*, 2020, **7**, 1420-1427.
36. M. Y. Yu, J. H. Liu, J. Yang and J. F. Ma, *J Alloy Compd*, 2021, **868**.
37. S. Hartung, N. Bucher, H. Y. Chen, R. Al-Oweini, S. Sreejith, P. Borah, Y. Zhao, U. Kortz, U. Stimming, H. E. Hoster and M. Srinivasan, *J Power Sources*, 2015, **288**, 270-277.
38. M. Zhang, A. M. Zhang, Y. F. Chen, J. Xie, Z. F. Xin, Y. J. Chen, Y. H. Kan, S. L. Li, Y. Q. Lan and Q. Zhang, *Energy Storage Mater*, 2020, **29**, 172-181.
39. D. F. Chai, C. J. Gomez-Garcia, B. N. Li, H. J. Pang, H. Y. Ma, X. M. Wang and L. C. Tan, *Chem Eng J*, 2019, **373**, 587-597.
40. E. Schreiber, N. A. Hartley, W. W. Brennessel, T. R. Cook, J. R. McKone and E. M. Matson, *Acs Appl Energ Mater*, 2019, **2**, 8985-8993.
41. A. M. Kosswattaarachchi, L. E. VanGelder, O. Nachtigall, J.

 

P. Hazelnis, W. W. Brennessel, E. M. Matson and T. R. Cook, *J Electrochem Soc*, 2019, **166**, A464-A472.

42. L. E. VanGelder, E. Schreiber and E. M. Matson, *J Mater Chem A*, 2019, **7**, 4893-4902.
43. B. E. Schurr, O. Nachtigall, L. E. VanGelder, J. Drappeau, W. W. Brennessel and E. M. Matson, *J Coord Chem*, 2019, **72**, 1267-1286.
44. O. W. Kolling, *Anal Chem*, 1982, **54**, 260-264.
45. G. Liu, Z. W. Zhao and A. Ghahreman, *Hydrometallurgy*, 2019, **187**, 81-100.
46. Y. Zhang, Y. H. Hu, L. Wang and W. Sun, *Miner Eng*, 2019, **139**.
47. X. Y. Zhao, M. H. Feng, Y. X. Jiao, Y. B. Zhang, Y. F. Wang and Z. L. Sha, *Desalination*, 2020, **481**.
48. W. Tahil, The Trouble with Lithium: Implications of Future PHEV Production for Lithium Demand).